Spatial filtering by a line-scanned nonrectangular detector: application to SPRITE readout MTF

Glenn D. Boreman and Allen E. Plogstedt

Any finite-sized photodetector has an effect on the spatial frequency content of the detected image. An expression for the modulation transfer function (MTF) of a nonrectangular detector in the along-scan direction is obtained. A comparison of our theoretical prediction is made with published experimental and numerical values for the MTF of a photosite having an exponentially tapered shape. Structures of this form are used as the readout region in SPRITE (signal processing in the element) detectors.

I. Introduction

Spatial filtering is commonly thought of as being implemented in the aperture plane of an optical system. However, spatial filtering may also occur in the image plane of an electronic imaging system, by virtue of the finite size of the individual detector elements. The modulation transfer function (MTF) of this process may be obtained from a consideration of the spatial averaging taking place over the surface of the photosite. An expression for the MTF of a scanning rectangular detector is derived, valid for the along-scan direction. The MTF expression is then generalized to include geometries where the photosite is nonrectangular.

A use of this formalism is then presented: a prediction of the MTF due to the readout geometry in a SPRITE (signal processing in the element) detector.[1-5] A SPRITE detector (Fig. 1) consists of a filament of photoconductive material in which a time delay and integration operation is performed on a scanned infrared image. The image data is read out as the voltage across a particular portion of the filament as a function of time. This photosensitive readout region of the SPRITE is often exponentially tapered to reduce the dispersion of carrier transit times in that region,[6] hence preserving the high frequency content of the image data.

In this paper, an alternative viewpoint on the mechanism of the tapered readout is presented, which allows an estimate of its MTF to be obtained directly from the readout geometry. The method of MTF calculation presented in Ref. 6 requires a numerical mapping of the electric field strength in the readout region. The prediction obtained from our model is compared with the results of that method and to published experimental MTF data for the particular readout structure of interest.

II. MTF of a Line-Scanned Rectangular Detector

The geometry under consideration is shown in Fig. 2. The image irradiance is $i(x,y)$ and the photosite responsivity function $d(x,y)$ is a rectangular function:

$$d(x,y) = \mathrm{rect}\left(\frac{x}{X}, \frac{y}{Y}\right). \tag{1}$$

The detector scans across the image with velocity v, converting the image data which falls on it into a time domain waveform. At an initial time $t = 0$, the response of the photosite may be written as

$$r(t=0) = \int_{-X/2}^{X/2}\int_{-Y/2}^{Y/2} i(x,y)\,dx\,dy. \tag{2}$$

At a general time t, the expression for photosite response generalizes to

$$r(t) = \int_{vt-X/2}^{vt+X/2}\int_{-Y/2}^{Y/2} i(x,y)\,dx\,dy. \tag{3}$$

Equation (3) may be recast in terms of a convolution of the image irradiance with the detector response.[7,8] Initially, we assume that the detector is free to scan in both the x and y directions, with velocities v_x and v_y. In that case, its response (as a function of the x-shift

Glenn Boreman is with University of Central Florida, Department of Electrical Engineering, Center for Research in Electro-Optics & Lasers, Orlando, Florida 32816; Allen Plogstedt is with McDonnell Douglas Astronautics Company, 701 Columbia Boulevard, Titusville, Florida 32780.

Received 6 July 1988.
0003-6935/89/061165-04$02.00/0.

variable $x_s = v_x t$ and the y-shift variable $y_s = v_y t$) would be

$$r(x_s,y_s) = \int_{x_s-X/2}^{x_s+X/2} \int_{y_s-Y/2}^{y_s+Y/2} i(x,y)dxdy, \tag{4}$$

$$r(x_s,y_s) = \iint_{-\infty}^{\infty} i(x,y)\ \mathrm{rect}\left[\frac{x-x_s}{X}, \frac{y-y_s}{Y}\right]dxdy, \tag{5}$$

$$r(x_s,y_s) = \iint_{-\infty}^{\infty} i(x,y)d(x-x_s,y-y_s)dxdy. \tag{6}$$

Thus, writing the 2-D convolution in Eq. (6) schematically:

$$r(x_s,y_s) = i(x,y) ** d(x,y). \tag{7}$$

Since the detector under consideration is actually only free to scan in the x direction, the detector response takes the form of

$$r(x_s,0) = \iint_{-\infty}^{\infty} i(x,y)d(x-x_s,y)dxdy, \tag{8}$$

which will later be useful to write as

$$r(x_s,0) = [i(x,y) ** d(x,y)] \times 1(x_s)\delta(y_s). \tag{9}$$

We may obtain $R(\xi)$, the 1-D Fourier transform of the detector response function $r(x_s,0)$ by means of the convolution theorem. We will consider a 1-D spatial transform where the scan variable x_s transforms to the ξ spatial frequency variable. This transformation may be thought of equivalently in the time/frequency domains as a transformation from the variable $v_x t$ to the variable f/v_x. Denoting the Fourier transform operator by $\mathcal{F}$:

$$R(\xi) = \mathcal{F}\{r(x_s,0)\}, \tag{10}$$

$$R(\xi) = \mathcal{F}\{[i(x,y) ** d(x,y)] \times 1(x_s)\delta(y_s)\}, \tag{11}$$

$$R(\xi) = [I(\xi,\eta) \times D(\xi,\eta)] ** \delta(\xi)1(\eta). \tag{12}$$

Writing the last expression in equivalent integral form yields

$$R(\xi) = \int_{-\infty}^{\infty} I(\xi,\eta) \times D(\xi,\eta)d\eta. \tag{13}$$

With $d(x,y) = \mathrm{rect}(x/X,y/Y)$, Eq. (13) reduces to

$$R(\xi) = \int_{-\infty}^{\infty} I(\xi,\eta)XY\ \mathrm{sinc}(X\xi,Y\eta)d\eta. \tag{14}$$

Finally, since $d(x,y)$ is separable for this example, $d(x,y) = d_x(x)d_y(y)$ and thus

$$d_x(x) \xrightarrow{\mathcal{F}} D_\xi(\xi) \text{ and } d_y(y) \xrightarrow{\mathcal{F}} D_\eta(\eta).$$

The expression for $R(\xi)$ yields

$$R(\xi) = XY\ \mathrm{sinc}(X\xi) \int_{-\infty}^{\infty} I(\xi,\eta)\ \mathrm{sinc}(Y\eta)d\eta. \tag{15}$$

Since the detector scans only in the x direction, we can obtain only ξ information in the Fourier domain of the signal. Since we cannot obtain η spectral information regarding the image data, a reasonable assumption to make is that $I(\xi,\eta)$ is separable [tantamount to assuming that the image data $i(x,y)$ was separable]. Under this assumption,

$$i(x,y) = i_x(x)i_y(y), \quad i_x(x) \xrightarrow{\mathcal{F}} I_\xi(\xi) \text{ and } i_y \xrightarrow{\mathcal{F}} I_\eta(\eta).$$

Thus, for Eq. (15) we can write

$$R(\xi) = XY\ \mathrm{sinc}(X\xi) \int_{-\infty}^{\infty} I_\xi(\xi)I_\eta(\eta)\ \mathrm{sinc}(Y\eta)d\eta, \tag{16}$$

$$R(\xi) = XY I_\xi(\xi)\ \mathrm{sinc}(X\xi) \int_{-\infty}^{\infty} I_\eta(\eta)\ \mathrm{sinc}(Y\eta)d\eta. \tag{17}$$

The MTF of the scanning detector system is the quantity of interest. The integral in Eq. (17) yields a constant which normalizes out in the usual definition of MTF. MTF relates the spectrum actually observed in the image $R(\xi)$ to the spectrum of the image incident on the detector $I(\xi)$. Thus the requirement that MTF be normalized to unity at zero spatial frequency yields

$$\mathrm{MTF}(\xi) = \frac{R(\xi)/I_\xi(\xi)}{R(\xi=0)}. \tag{18}$$

For the case of a 1-D scanning rectangular detector of width X,

$$\mathrm{MTF}(\xi) = D_\xi(\xi)/D_\xi(\xi=0) = \mathrm{sinc}(X\xi). \tag{19}$$

Thus, for the case of a separable photosite function, the MTF in the ξ direction was only affected by the x-profile of the photosite responsivity. The following section shows that, for a nonseparable photosite re-

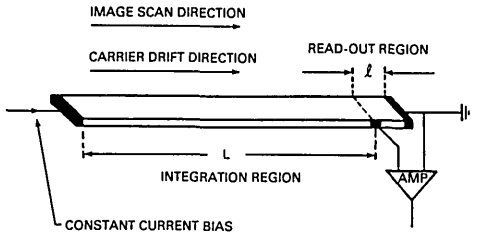

Fig. 1. Basic structure of the SPRITE detector. The image is scanned mechanically in the same direction as the carrier drift, enhancing the signal-to-noise ratio of the resulting image.

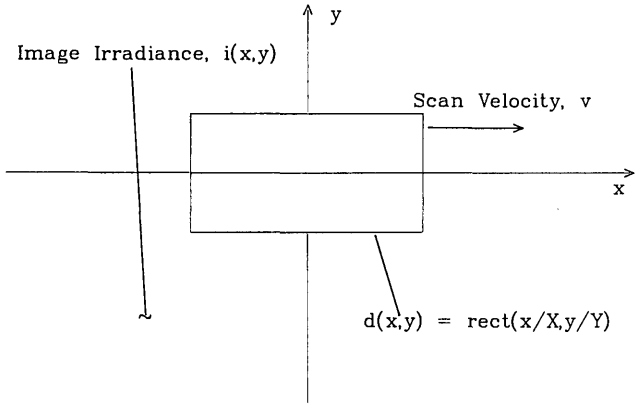

Fig. 2. Geometry for the scanned rectangular detector.

sponsivity $d(x,y)$, the MTF in the ξ direction depends on the y-profile of the responsivity function also.

III. MTF of a Line-Scanned Nonrectangular Detector

In this section we consider the more general image scanning geometry of Fig. 3, where the photosite responsivity function $d(x,y)$ is a nonseparable function of the x and y coordinates. In this case, it is not possible to express $d(x,y)$ as a product of two functions, one solely dependent on x and one solely dependent on y. The photosite responsivity is again assumed to be a one-zero function, i.e., equal to unity inside and equal to zero outside. We also assume that it is symmetric about the x-axis. With these assumptions, Eq. (13) still holds for an x-direction scan:

$$R(\xi) = \int_{-\infty}^{\infty} I(\xi,\eta) \times D(\xi,\eta)d\eta. \tag{20}$$

Making the same assumption as in the last section with regard to the separability of the image data,

$$R(\xi) = I_\xi(\xi) \int_{-\infty}^{\infty} I_\eta(\eta)D(\xi,\eta)d\eta. \tag{21}$$

To obtain an expression for MTF(ξ), the 2-D function $D(\xi,\eta)$ need only be evaluated along the ξ axis:

$$R(\xi) = I_\xi(\xi) \int_{-\infty}^{\infty} I_\eta(\eta)D(\xi,0)d\eta, \tag{22}$$

$$R(\xi) = I_\xi(\xi)D(\xi,0) \int_{-\infty}^{\infty} I_\eta(\eta)d\eta. \tag{23}$$

The final integral will again normalize out under the usual definition for MTF:

$$\mathrm{MTF}(\xi) = \frac{R(\xi)/I_\xi(\xi)}{R(\xi = 0)}, \tag{24}$$

$$\mathrm{MTF}(\xi) = D(\xi,0)/D(0,0). \tag{25}$$

For the present case of nonseparable $d(x,y)$, note that

$$D(\xi,0) \neq \mathcal{F}\{d(x,0)\}. \tag{26}$$

Hence, the y-dependence of the responsivity function affects the ξ-profile of the transform, and therefore the ξ-domain (along-scan) MTF as well.

The problem of determining the impact of detector shape on the along-scan MTF reduces to finding the ξ-axis profile of the 2-D Fourier transform of the one-zero function $d(x,y)$. For the detector geometry shown in Fig. 3, for the transform of $d(x,y)$ we can write[9,10]

$$D(\xi,\eta) = \iint_{-\infty}^{\infty} d(x,y) \exp(-j2\pi\xi x) \exp(-j2\pi\eta y)dxdy. \tag{27}$$

Using the fact that $d(x,y)$ is a zero-one function:

$$D(\xi,\eta) = \int_{-\infty}^{\infty} \exp(-j2\pi\xi x) \int_{-y(x)}^{y(x)} \exp(-j2\pi\eta y)dydx. \tag{28}$$

For the case of interest to our application, the value of the transform along $\eta = 0$ yields

$$D(\xi,0) = \int_{-\infty}^{\infty} \exp(-j2\pi\xi x) \int_{-y(x)}^{y(x)} dydx, \tag{29}$$

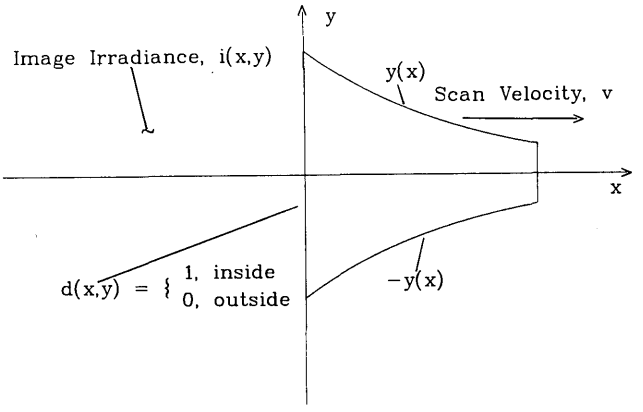

Fig. 3. Geometry for the scanned nonrectangular detector.

$$D(\xi,0) = \int_{-\infty}^{\infty} \exp(-j2\pi\xi x)2y(x)dx = 2Y(\xi). \tag{30}$$

Thus, the y-profile of the photosite response function comes explicitly into the calculation of the MTF in the ξ-direction. The formulation of Eq. (25) yields

$$\mathrm{MTF}(\xi) = D(\xi,0)/D(0,0) = Y(\xi)/Y(0). \tag{31}$$

Referring to Fig. 3, we have a function $y(x)$ of the form

$$y(x) = \mathrm{rect}\left(\frac{x - X/2}{X}\right) \exp(-\alpha x). \tag{32}$$

The resulting MTF expression in the ξ-direction is

$$\mathrm{MTF}(\xi) = Y(\xi)/Y(0) \propto \mathcal{F}\left[\mathrm{rect}\left(\frac{x - X/2}{X}\right) \exp(-\alpha x)\right]. \tag{33}$$

Because of the convolution theorem, the MTF of the tapered scanning detector will be wider than the MTF of an untapered detector, i.e.,

$$\mathcal{F}\left[\mathrm{rect}\left(\frac{x - X/2}{X}\right) \exp(-\alpha x)\right] = \mathcal{F}\left[\mathrm{rect}\left(\frac{x - X/2}{X}\right)\right] * \mathcal{F}[\exp(-\alpha x)]. \tag{34}$$

The function described by Eq. (34) will have a greater equivalent width than will the function $\mathcal{F}[\mathrm{rect}(x/X)]$.

In the next section we use our method to predict the difference in MTF between two different photosite geometries: rectangular vs a structure with an exponential taper. This prediction will then be compared to previously published MTF results for such structures.

IV. Comparison to Previously Published MTF Results

In this section we predict the difference in MTF between two photosite geometries which are used as readout structures in SPRITE detectors. One such structure is a rectangular readout 50 μm long and 35 μm wide, and the other is an exponentially tapered readout which is 62.5 μm at the wide end, 50 μm long, and 15 μm wide at the short end. This prediction is then compared to previously published numerical and experimental MTF results for such structures.

Expressions for $y(x)$, the y-profile of the respective photosite responses, are as follows:

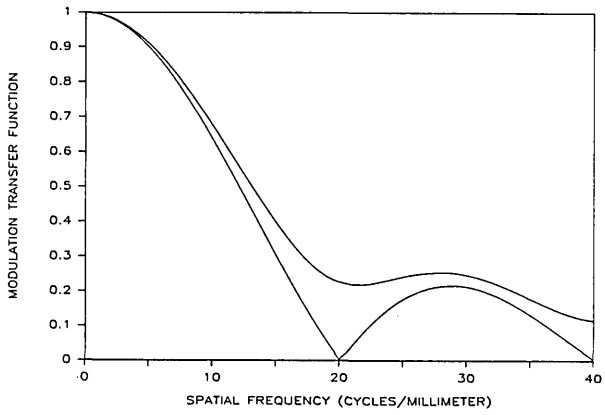

Fig. 4. Comparison of MTFs for rectangular (lower curve) and tapered (upper curve) photosites.

$$y_{\text{rect}}(x) = \text{rect}\left(\frac{x-25}{50}\right) \tag{35}$$

$$y_{\text{taper}}(x) = \text{rect}\left(\frac{x-25}{50}\right) \times \exp(-\alpha x), \tag{36}$$

where α may be found from the equation for the taper

$$62.5 \exp(-\alpha 50) = 15; \quad \alpha = 0.0285. \tag{37}$$

The magnitudes of the normalized Fourier transforms of the functions from Eqs. (35) and (36) are plotted in Fig. 4. These plots correspond to the ξ-axis (along-scan direction) MTFs for the two readout structures. Comparing these curves, it is seen that the tapered readout geometry should have a wider MTF (at the $1/e$ point) by $\approx$12%.

A numerical simulation of these structures was carried out in Ref. 6, where a map of the electric field inside the readout was made. The carrier transit time was computed along each streamline, and the spread in transit times was used to predict the width of the impulse response. The difference in the impulse response widths (at the $1/e$ points) for the two structures was predicted to be $\approx$43% using that technique.

Experimental MTF data comparing these structures is found in Refs. 6 and 11. There is some variability in the measured data, but the two readout structures were found to differ by $\approx$15–20% in impulse response widths at $1/e$ points.

The MTF results from the geometrical convolution method presented herein are seen to be in closer agreement with the measured values than are the results of the numerical E-field mapping method.

V. Conclusions

A geometrical method has been presented for the calculation of along-scan MTF values for line-scanned detectors which are nonrectangular in shape. The shape of the photosite in the perpendicular-to-scan direction was found to affect the MTF in the along-scan direction. This is due to the nonseparability of the detector geometry. The predictions of this model were compared with published experimental values and found to be in closer agreement than previous models.

In the analysis of SPRITE detectors, considering the action of the readout to be a convolutional process applied to the image data has the advantage that the MTF is easily obtained from a consideration of the geometry of the structure.

This geometrical theory was developed without regard for carrier recombination effects in the readout region. Thus, it would be expected that the results of this method would be most valid in cases where the mean carrier drift length before recombination was long compared to the total length of the readout. Also, any inherent MTF due to carrier diffusion effects would multiply the readout MTF and would tend to decrease the observed difference between various readout geometries.

Finally, it should be noted that the possibility exists for tailoring the shape of a scanning detector to emphasize certain spatial frequencies in the image data. However, for a given envelope dimension of the photosite, this emphasis will be at the expense of the overall magnitude of the response.

This work was supported by McDonnell Douglas Astronautics Co., Titusville Division, and by the Center for Research in Electro-Optics & Lasers of the University of Central Florida.

References

1. C. T. Elliott, "New Detector for Thermal Imaging Systems," Electron. Lett. **17**, 312 (1981).
2. C. T. Elliott, D. Day, and D. J. Wilson, "An Integrating Detector for Serial Scan Thermal Imaging," Infrared Phys. **22**, 31 (1982).
3. A. Blackburn, M. V. Blackman, D. E. Charlton, W. A. E. Dunn, M. D. Jenner, K. J. Oliver, and J. T. M. Wotherspoon, "The Practical Realization and Performance of SPRITE Detectors," Infrared Phys. **22**, 57 (1982).
4. D. J. Day and T. J. Shepherd, "Transport in Photo-Conductors—I," Solid State Electron. **25**, 707 (1982).
5. G. Boreman and A. Plogstedt, "Modulation Transfer Function and Number of Equivalent Elements for SPRITE Detectors," Appl. Opt. **27**, 4331 (1988).
6. T. Ashley, C. T. Elliott, A. M. White, J. T. M. Wotherspoon, and M. D. Johns, "Optimization of Spatial Resolution in SPRITE Detectors," Infrared Phys. **24**, 25 (1984).
7. J. M. Lloyd, *Thermal Imaging Systems* (Plenum, New York, 1975), Chap. 9.
8. L. G. Callahan and W. M. Brown, "One- and Two-Dimensional Processing in Line Scanning Systems," Appl. Opt. **2**, 401 (1963).
9. A. Papoulis, *Systems and Transforms with Applications in Optics* (McGraw-Hill, New York, 1968), pp. 95–96.
10. J. D. Gaskill, *Linear Systems, Fourier Transforms and Optics* (Wiley, New York, 1978), pp. 311–312.
11. S. P. Braim and A. P. Campbell, "TED (SPRITE) Detector MTF," in *Proceedings of the Conference on Advanced IR Detectors and Systems* (IEE, London, 1983), Vol. 228, p. 63.